Optics Letters

Digital four-step phase-shifting technique from a single fringe pattern using Riesz transform

Yassine Tounsi,[1,†] Manoj Kumar,[2,†] Ahmed Siari,[1] Fernando Mendoza-Santoyo,[3] Abdelkrim Nassim,[1,*] and Osamu Matoba[2]

[1]Sciences Faculty, Department of Physics, ChouaibDoukkali University, Benmaachou Street, El Jadida 24000, Morocco
[2]Department of Systems Science, Graduate School of System Informatics, Kobe University, Rokkodai 1-1, Nada, Kobe 657-8501, Japan
[3]Centro de Investigaciones en Optica, A.C., Leon, Guanajuato 37160, Mexico
*Corresponding author: nassim.a@ucd.ac.ma

Received 2 May 2019; revised 27 May 2019; accepted 3 June 2019; posted 10 June 2019 (Doc. ID 366679); published 8 July 2019

A digital four-step phase-shifting method for obtaining the optical phase distribution from a single fringe pattern is proposed in this Letter. By computing the first-, second-, and third-order Riesz transform components for a given fringe pattern, three $\pi/2$ phase-shifted fringe patterns are generated from the obtained Riesz components and, finally, the wrapped phase map is extracted. The validity of the proposed method is demonstrated on both the simulated and experimentally obtained fringe patterns. The performance of the proposed method is evaluated by using the image quality index and edge preservation index. Further, the performance of the proposed method is tested on speckled correlation fringes obtained from digital speckle pattern interferometry, and the resulting phase from the proposed method is compared with the phase obtained from three experimentally recorded phase-shifted fringe patterns. The obtained results reveal that the proposed method provides a simple and robust solution for optical phase extraction from a single fringe pattern with good accuracy and, therefore, make it suitable for real-time measurement applications.

https://doi.org/10.1364/OL.44.003434

Over the years, interferometric techniques such as digital speckle pattern interferometry (DSPI) and digital holographic interferometry, have been playing a major role in solving a rather large number of problems for scientific, engineering, and industrial applications, namely, the determination of materials properties, nondestructive testing of materials, structural analysis, experimental mechanics for strain, displacement evaluation [1–7], etc. The desired physical parameter to be measured is related to the phase map encoded in the intensity distribution of the recorded fringe pattern. Various techniques/methods have been proposed to retrieve and evaluate this optical phase. These are classified mainly in two important families: the first is the phase-shifting technique which is used to record more than one phase-shifted fringe pattern [7–10], while the second exploits a single fringe pattern from which the desired phase distribution is found. The conventional phase-shifting techniques have been widely used in many areas of precise interferometric metrology, but they face some crucial drawbacks such as being quite susceptible to atmospheric turbulence and, hence, more sensitive to environmental disturbances. Moreover, these techniques are difficult to implement in the study of dynamic and fast transient phenomena, and make the system more complicated and error-prone. A single-shot parallel phase-shifting interferometry from a single interferogram was proposed [11], providing promising results for the investigations of dynamic events [12]. The phase evaluation from a single fringe pattern can be realized by either of two methods: the first introduces a high-frequency spatial carrier to generate a modulated fringe pattern, and then demodulate it in the frequency domain using Fourier or wavelets transform [13–15]. The second extracts the phase without introducing a spatial carrier using a monogenic signal [3–5,16].

Takeda *et al.* [13] proposed the analysis of interferograms in the Fourier domain by computing its Fourier transform, whose band filter needs to be built in many cases to enhance the signal-to-noise ratio. Other researchers exploit wavelets domain to demodulate the interferograms: Ghlaifan *et al.* [14] exploit discrete wavelet transforms by using Gabor's function as the mother wavelet, whereas Affifi *et al.* [15] applies the continuous wavelets transform using Paul's wavelets. For the wavelet transform, the mother wavelet function, its scale and shift parameter need to be found in advance to obtain a better-recovered phase information. Besides these, the works in Refs. [3–5] exploit the monogenic signal theory to retrieve the phase distribution from digital speckle pattern interferometric (DSPI) fringes.

In this Letter, we propose a digital four-step phase-shifting method (D4-PS) based on the first-, second-, and third-order Riesz transform for the extraction of the phase distribution from a single fringe pattern. The Riesz transform is the two-dimensional extension of the Hilbert transform [16]. We consider a fringe pattern with intensity distribution denoted as $f(x,y)$ and expressed as

$$f(x,y) = a(x,y) + b(x,y) \cdot \cos \varphi(x,y), \tag{1}$$

where $a(x,y)$ is an intensity bias, $b(x,y)$ is the visibility, and $\varphi(x,y)$ is the phase distribution containing the desired

information. The first-order Riesz kernels of a fringe pattern along the x- and y-directions are defined, respectively, as

$$r_x = \frac{-x}{2\pi(x^2+y^2)^{3/2}}; \quad r_y = \frac{-y}{2\pi(x^2+y^2)^{3/2}}. \tag{2}$$

The first-order Riesz transform of the fringe pattern $f(x,y)$ is computed as

$$R^1(f(x,y)) = \begin{cases} f_1 = r_x * f(x,y) \\ f_2 = r_y * f(x,y) \end{cases}, \tag{3}$$

where R^1 represents the first-order Riesz operator, * stands for the convolution product, and f_1, f_2 are the horizontal and vertical Riesz components for the input fringe pattern, $f(x,y)$.

The second-order Riesz transform of the input fringe pattern $f(x,y)$ is computed as

$$R^2(f(x,y)) = \begin{cases} f_3 = r_x * (r_x * f(x,y)) \\ f_4 = r_y * (r_x * f(x,y)) \\ f_5 = r_y * (r_y * f(x,y)) \end{cases}, \tag{4}$$

where R^2 represents the second-order Riesz operator. f_3, f_4, and f_5 are the second-order Riesz components of the input fringe pattern.

The third-order Riesz transform is computed as

$$R^3(f(x,y)) = \begin{cases} f_6 = r_x * r_x * (r_x * f(x,y)) \\ f_7 = r_x * r_x * (r_y * f(x,y)) \\ f_8 = r_x * r_y * (r_y * f(x,y)) \\ f_9 = r_y * r_y * (r_y * f(x,y)) \end{cases}, \tag{5}$$

where R^3 represents the third-order Riesz operator. f_6, f_7, and f_8 and f_9 are the third-order Riesz components of the input fringe pattern.

The first-, second-, and the third-order Riesz transform components, respectively, provide two, three, and four components, in accordance with the Riesz transform theory that states that the nth-order Riesz transform gives $n+1$ components [16]. Thus, from the three Riesz transform orders (R^1, R^2, and R^3) of the input/single fringe pattern, nine components, $f_1(x,y)$, $f_2(x,y)$, $f_3(x,y)$, $f_4(x,y)$, $f_5(x,y)$, $f_6(x,y)$, $f_7(x,y)$, $f_8(x,y)$, and $f_9(x,y)$, are obtained. Using the following equations to combine the components for each order result in three $\pi/2$ shifted fringe patterns:

$$f(x,y,\pi/2) = a(x,y) - b(x,y)\cdot\sin\varphi(x,y) = \mathrm{sgn}(u)\cdot\sqrt{f_1^2+f_2^2}, \tag{6a}$$

$$f(x,y,\pi) = a(x,y) - b(x,y)\cdot\cos\varphi(x,y) = \mathrm{sgn}(v)\cdot(f_3+f_5), \tag{6b}$$

$$f(x,y,3\pi/2) = a(x,y) + b(x,y)\cdot\sin\varphi(x,y) = \mathrm{sgn}(w)\cdot\sqrt{f_6^2+f_9^2}, \tag{6c}$$

where $u = f_1, f_2$, $v = f_3, f_4, f_5$, $w = f_6, f_7, f_8, f_9$, and 'sgn' is the sign (signum) function defined as

$$\mathrm{sign}(x) = \begin{cases} -1; x < 0 \\ 0; x = 0 \\ 1; x > 0 \end{cases}. \tag{7}$$

The proposed method to obtain three phase-shifted fringe patterns from a single fringe pattern using the Riesz transform is schematically explained in Fig. 1 so that, together with the original input fringe pattern, four shifted patterns are available. The modulo 2π phase distribution is evaluated by

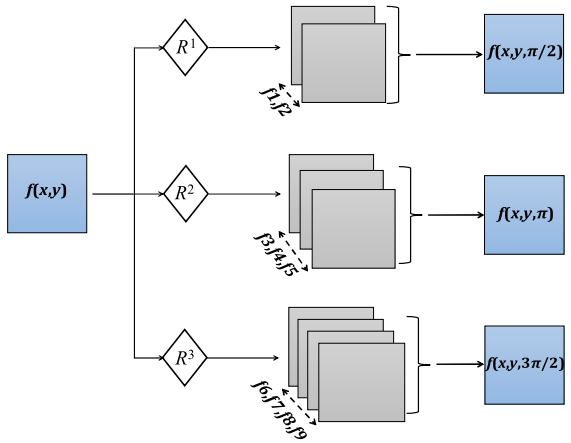

Fig. 1. Explaining the scheme of the proposed technique.

$$\varphi(x,y) = \arctan\left(\frac{f(x,y,3\pi/2) - f(x,y,\pi/2)}{f(x,y,0) - f(x,y,\pi)}\right). \tag{8}$$

The method is verified first on a simple fringe pattern, shown in Fig. 2, simulated using a linear phase distribution whose corresponding cross-sectional plot is shown at the bottom. Figure 3 (right column) shows the resulting three $\pi/2$ phase-shifted fringe patterns obtained by using the proposed method, along with their cross-sectional plots. Figure 3 (left column) shows the real $\pi/2$ phase-shifted fringe patterns with their cross-sectional plots.

The original fringe pattern and the obtained three $\pi/2$ phase-shifted patterns are used to extract, through Eq. (8), the wrapped phase distribution shown in Fig. 4(a). Figure 4(b) shows the wrapped phase obtained from the three real phase-shifted fringe patterns, shown in Fig. 3 (left column). The wrapped phase distribution is continuous between 0 and 2π with the phase discontinuity removed using the phase unwrapping max-flow algorithm (PUMA) [17]. The continuous unwrapped phase for Fig. 3 (right column) is shown in Fig. 4(c), while Fig. 4(d) presents the real unwrapped phase distribution for the real $\pi/2$ phase-shifted fringe patterns shown in Fig. 3 (left column). The plots of the wrapped and unwrapped phases for both cases along line AB are shown in Fig. 4(e), showing that the obtained phase distribution from

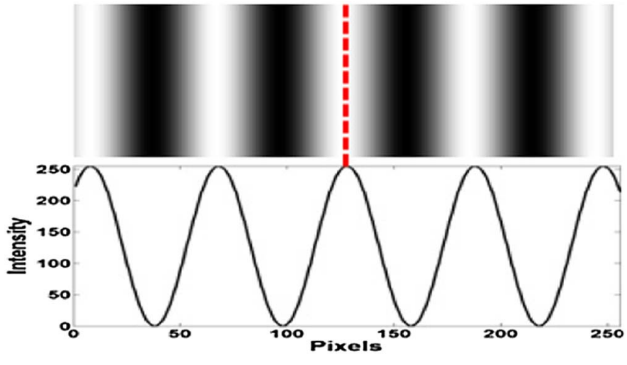

Fig. 2. Simulated fringe pattern and its corresponding cross section.

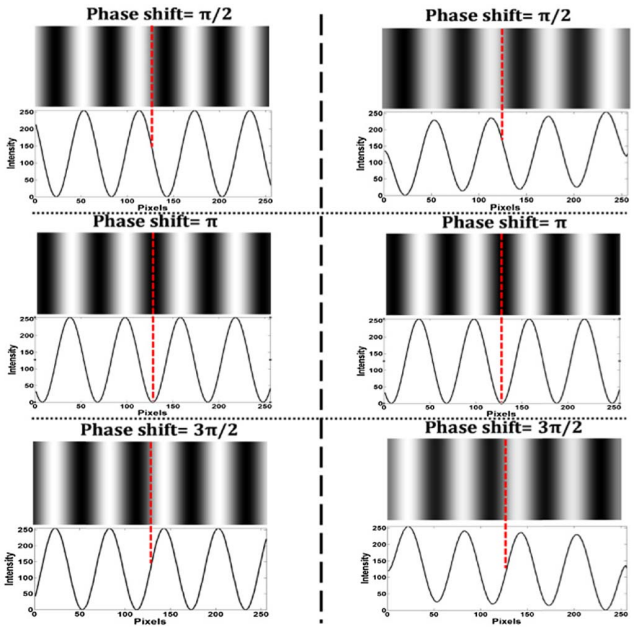

Fig. 3. Shifted fringe patterns and their corresponding cross-sectional plots. Left column: real phase-shifted fringe patterns. Right column: phase-shifted fringe patterns generated using the Riesz transform method.

the proposed method is in very good agreement with the actual (real) phase distribution. A phase error of 0.63 is calculated between the phase obtained with the proposed method and the corresponding real phase. Moreover, for completeness, the performance of obtaining the phase distributions from a single fringe pattern by the proposed method is quantified by two criteria: the quality (Q) index and the edge preservation index (EPI) [18]. The Q index measures the image distortion by taking into account the loss of correlation, luminance distortion, and contrast distortion between two images. The Q index takes the values between −1 and 1, where $Q = 1$ means that f and f_{out} are similar and 100% correlated. On the other hand, EPI measures the edge preservation; its value is in the range [0,1], where 1 is satisfied for an exact edge. The ratio Q/EPI obtained in this case are 0.968/0.981, 1/1, 0.986/0.991, and 0.987/0.999, respectively, for $\pi/2$, π and $3\pi/2$ phase-shifted fringes, and the retrieved wrapped phases, respectively.

The performance of the proposed method is also evaluated by considering several simulated fringe patterns shown in

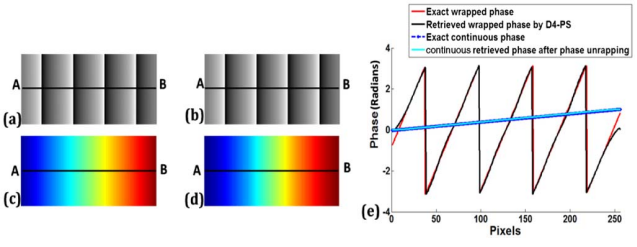

Fig. 4. Retrieved phase using (a) the proposed method and (b) the real phase. The unwrapped phase map corresponding to (c) Fig. 4(a) and (d) Fig. 4(b). (e) Plots of the wrapped and unwrapped phases for both the cases along line AB.

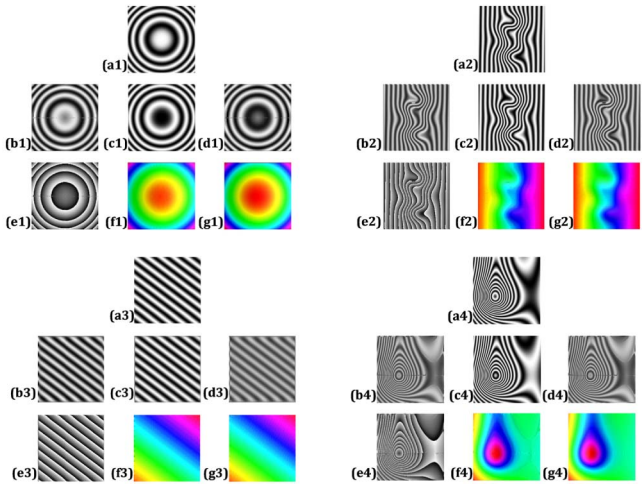

Fig. 5. (a1)–(a4) Input fringe patterns, (b1)–(b4) $\pi/2$, (c1)–(c4) π, and (d1)–(d4) $3\pi/2$ phase-shifted fringe patterns. (e1)–(e4) are the retrieved phase distributions using the proposed D4-PS method. (f1)–(f4) are the continuous retrieved phase distributions. (g1)–(g4) are the real phase distributions.

Figs. 5(a1)–5(a4), 5(b1)–5(b4), 5(c1)–5(c4), and 5(d1)–5(d4), respectively, which show the input fringe patterns, $\pi/2$, π, and $3\pi/2$ phase-shifted fringe patterns obtained from the proposed method. Figures 5(e1)–5(e4) show the obtained wrapped phase distributions, and Figs. 5(f1)–5(f4) show the corresponding unwrapped phase distributions obtained by using the proposed method, whereas Figs. 5(g1)–5(g4) show the real unwrapped phase distributions.

Furthermore, the proposed method is evaluated on fringe patterns experimentally obtained using DSPI, which has been considered as a powerful technique for non-contact characterization of materials surfaces and physical parameter measurements [3–5]. Figure 6(a) shows a simulated speckle fringe pattern. As it is well known, DSPI data are characterized by residual speckle noise that influences the analysis step and, for this reason, we used a recently proposed method based on the Riesz wavelets transform thresholding technique to filter the speckle noise from the DSPI fringe patterns [19]. The denoised DSPI fringe pattern is shown in Fig. 6(b). Figures 6(c)–6(e) show the three $\pi/2$ phase-shifted fringe patterns obtained by the proposed method, and Fig. 6(f) shows the obtained wrapped distribution corresponding to the fringe

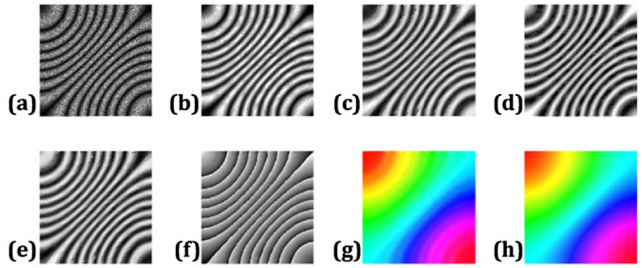

Fig. 6. Results of the proposed method on simulated DSPI fringe pattern. (a) Simulated DSPI fringe pattern. (b) Denoised fringe pattern. (c–e) $\pi/2$, π, and $3\pi/2$ phase-shifted fringe patterns using the proposed method. (f) Retrieved wrapped phase distribution map. (g) Continuous retrieved phase. (h) Real phase distribution map.

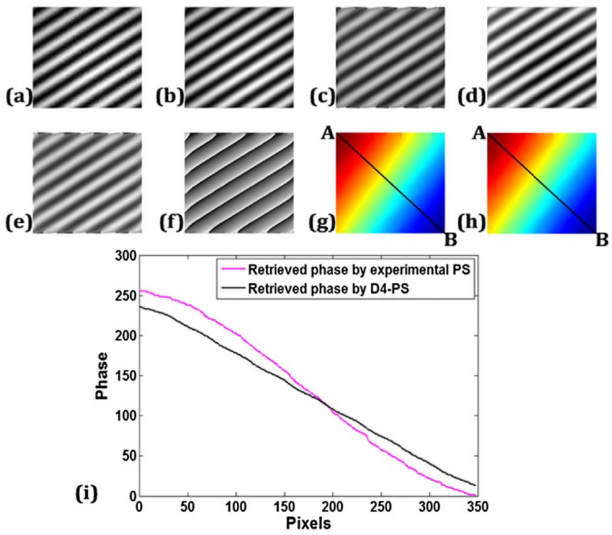

Fig. 7. (a) Experimental DSPI data. (b) Denoised experimental DSPI data. (c)–(e) Three $\pi/2$ shifted speckle fringe pattern. (f) Retrieved phase. (g) Continuous retrieved phase using the PUMA. (h) Provided phase distribution by 4D Technology obtained from experimental $\pi/2$ shifted speckle fringe patterns. (i) Plots of unwrapped phases for both the cases (g)–(h) along line AB.

pattern of Fig. 6(a). The obtained and real unwrapped phase maps of the DSPI fringe patterns are shown in Figs. 6(g) and 6(h), respectively. The denoising of the DSPI fringe pattern is done in order to obtain the phase distribution with good accuracy.

The performance of the proposed method is evaluated on the basis of the Q index and EPI. The obtained metric values show that the proposed method is robust and effective for evaluating the phase information from a single fringe pattern in digital interferometric techniques.

Finally, the experimental evaluation of the proposed method was tested on the fringe pattern shown in Fig. 7(a) (kindly provided by 4D Technology), obtained by DSPI while looking at an aluminium transducer suspension assembly from a hard disk drive. Figure 7(b) shows the filtered fringe pattern; Figs. 7(c)–7(e) show the three $\pi/2$ phase-shifted speckle fringe patterns, and Fig. 7(f) shows the wrapped phase distribution map obtained with Eq. (8). The unwrapped phase distribution map is shown in Fig. 7(g) which is almost identical to the unwrapped phase distribution map obtained from three $\pi/2$ phase-shifted fringe patterns experimentally recorded and provided by the 4D Technology. Figure 7(i) shows the plots along the line AB for both unwrapped phase distributions.

In summary, a digital D4-PS method is proposed that is able to extract the phase distribution from a single fringe pattern. The phase shifting is realized digitally by computing the first-, second-, and third-order Riesz transform components of the single fringe pattern. Nine Riesz components are obtained and combined to generate three $\pi/2$ phase-shifted fringe patterns. The simulation results show that the D4-PS method provides promising results quantified in terms of the Q and EPI image metrics. The performance of the proposed D4-PS method is verified on various fringe types. Additionally, the performance of the method is demonstrated on experimental DSPI data, where the retrieved phase is compared with the obtained phase by using phase-shifting interferometry, and it is found that the proposed method provides the phase information with high accuracy. The proposed method is reliable and can replace the conventional phase-shifting techniques which are more expensive, sensitive to vibration and turbulence, and time-consuming when it comes to calibrating the hardware to perform the phase-shifting procedure.

Funding. Japan Society for the Promotion of Science (JSPS) (17F17370, 18H03888); Japan Science and Technology Agency (JST) (JPMJCR1755).

Acknowledgment. The authors want to thank Dr. N. Brock and Prof. J. C. Wyant from 4D Technology for providing the experimentally shifted fringe patterns. M. Kumar and O. Matoba acknowledge the support by JSPS KAKENHI and JST CREST.

†These authors contributed equally to this Letter.

REFERENCES

1. P. K. Rastogi, *Optical Measurement Techniques and Applications* (Artech House, 1997).
2. P. K. Rastogi, *Photomechanics, Topics in Applied Physics* (Springer, 2000).
3. M. Kumar, S. Agarwal, V. Kumar, G. S. Khan, and C. Shakher, Appl. Opt. **54**, 2450 (2015).
4. M. Kumar and C. Shakher, Opt. Lasers Eng. **73**, 33 (2015).
5. M. Kumar, R. Agarwal, R. Bhutani, and C. Shakher, Opt. Eng. **55**, 054101 (2016).
6. M. Kumar and C. Shakher, Appl. Opt. **55**, 960 (2016).
7. P. de Groot, *Optical Measurement of Surface Topography*, R. Leach, ed. (Springer, 2011), pp. 167–186.
8. I. Yamaguchi and T. Zhang, Opt. Lett. **22**, 1268 (1997).
9. W. Zhou, Q. Xu, Y. Yu, and A. Asundi, Opt. Lasers Eng. **47**, 896 (2009).
10. W. Zhou, H. Zhang, and T. C. Poon, IEEE Trans Ind. Informat. **12**, 1564 (2016).
11. Y. Awatsuji, M. Sasada, and T. Kubota, Appl. Phys. Lett. **85**, 1069 (2004).
12. T. Kakue, R. Yonesaka, T. Tahara, Y. Awatsuji, K. Nishio, S. Ura, T. Kubota, and O. Matoba, Opt. Lett. **36**, 4131 (2011).
13. M. Takeda, H. Ina, and S. Kobayashi, J. Opt. Soc. Am. **72**, 156 (1982).
14. A. Ghlaifan, Y. Tounsi, S. Zada, D. Muhire, and A. Nassim, Opt. Eng. **55**, 121708 (2016).
15. M. Afifi, A. Fassi-Fihri, M. Marjane, K. Nassim, M. Sidki, and S. Rachafi, Opt. Commun. **211**, 47 (2002).
16. E. M. Stein and G. Weiss, *Introduction to Fourier Analysis on Euclidean Spaces (PMS-32)* (Princeton University, 1971).
17. J. M. Bioucas-Dias and G. Valadao, IEEE Trans. Image Process **16**, 698 (2007).
18. Z. Wang and A. C. Bovik, IEEE Signal Process. Lett. **9**, 81 (2002).
19. T. Yassine, S. Ahmed, and N. Abdelkrim, *International Conference on Advanced Technologies for Signal and Image Processing (ATSIP)* (2017), pp. 1–4.